Talanta 112 (2013) 117–122

Contents lists available at SciVerse ScienceDirect

Talanta

journal homepage: www.elsevier.com/locate/talanta

Highly selective and sensitive detection of coralyne based on the binding chemistry of aptamer and graphene oxide

Pu Zhang [a,c], Yi Wang [b], Fei Leng [b], Zu Hong Xiong [c], Cheng Zhi Huang [a,b,*]

[a] Education Ministry Key Laboratory on Luminescence and Real-Time Analysis, College of Pharmaceutical Sciences, Southwest University, Chongqing 400715, China
[b] College of Chemistry and Chemical Engineering, Southwest University, Chongqing 400715, China
[c] College of Physical Science and Technology, Southwest University, Chongqing 400715, China

ARTICLE INFO

Available online 13 March 2013

Keywords:
Graphene
Aptamer
Organic small molecule
Coralyne
Fluorescence

ABSTRACT

In this contribution, an organic small molecule (OSM)-participating interaction between its aptamer and graphene oxide (GO) is investigated by taking coralyne as an example. Based on their interactions, a simple, rapid, highly sensitive and selective fluorometric method for the detection of coralyne is developed. GO can effectively quench the fluorescence of dye-labeled aptamer, while stronger binding of the aptamer and its target can make the fluorescence be recovered, which have been well demonstrated by the studies of the fluorescence spectra, fluorescence anisotropy, and circular dichroism spectra. In this case, the coralyne can be quantificationally detected by the variation of the fluorescence intensity, where GO acts as an efficient signal-to-background enhancer. With the increase of the coralyne, the fluorescence intensity increases gradually and linearly proportional to the concentration of the coralyne in the range of 10–700 nmol L^{-1}. This method is reliable, and has been successfully applied for the detection of coralyne in complicated matrixes.

1. Introduction

Over the past decade, developing analytical methods with the advantages of *Simple*, *Speedy*, *Sensitive*, and *Selective* features, combined with *Automatic* operation, *Accurate*, and *Efficient* outputs (so-called 4S+2A+E) has attracted increasing attention. The established methods with these advantages have played important roles in a variety of different areas related to environmental monitoring, food analysis, clinic diagnosis, and drug quality control [1]. Although a large number of methods have been successfully demonstrated for the detection of a specific target, however, most of them suffer from the limitations such as time-consuming, cumbersome, low sensitivity and selectivity, and poor performance in complex matrixes. Taking organic small molecules (OSMs) as an example, there are several challenges during their detection by the optical methods: (i) most of the OSMs do not have any optical signals in UV or visible region, and thus they can hardly be monitored by their own signals; (ii) the strategies for the assay which depend on the intermolecular forces (*e.g.*, electrostatic interaction or Van der Waals force) between the probes and OSMs are usually with low-selectivity and high-background signals [2–4]; (iii) design and synthesis of specific molecular probes for the recognition of OSMs via coordination or covalent bonds can achieve high selectivity and sensitivity, however, these probes cannot be widely extended to other systems. Therefore, developing simple, rapid, highly sensitive and selective, and general platforms for the detection of OSMs is still a grand challenge.

Recently, graphene has attracted increasing attention due to its unique structure and properties. Owing to its high quenching efficiency to the fluorescence, graphene has been developed as nanoplatforms in optical detections, especially for fluorescence resonance energy transfer [5–7]. Based on the change of optical signals, these graphene-involved systems have been used for DNA and protein analysis, metal ions detection, single bacterium detection, drug delivery, and biological imaging [8–14]. Therefore, it is easy to develop high-performance sensing platforms consisted of graphene with high quenching efficiency and a specific recognition system with high affinity to the target. To this end, aptamer is used as a recognition element to achieve the high affinity and selectivity toward the target in the present work. Aptamer is selected from a large number of random sequences of oligonucleotides or peptides, and can specifically bind to its target with high binding constant [15]. Aptasensors for the recognition of small molecules, proteins and cancer cells also have been developed in recent years due to the specific binding affinities to their targets [16].

Herein, coralyne, a kind of alkaloid, is used as a model OSM to investigate the interaction among graphene oxide (GO), OSM and its aptamer. It has been demonstrated that coralyne can restrict the leukemia growth in cells and exhibit a noticeable antitumor activity, and thus a promising new medicine for the cancer therapy [17,18].

* Corresponding author at: Education Ministry Key Laboratory on Luminescence and Real-Time Analysis, College of Pharmaceutical Sciences, Southwest University, Chongqing 400715, China.
Tel.: +86 23 68254659; fax: +86 23 68367257.
E-mail address: chengzhi@swu.edu.cn (C.Z. Huang).

0039-9140/$ - see front matter © 2013 Elsevier B.V. All rights reserved.
http://dx.doi.org/10.1016/j.talanta.2013.03.013

As such, quality control and quantitive detection of coralyne *in vivo* and *in vitro* is of great importance. To date, there have been only a few reports on the detection of coralyne. One example was the colorimetric detection of coralyne with gold/silver nanoparticles as probes [19,20]. In these cases, aggregation of metal nanoparticles might occur and result in high background signals and low sensitivity, and these methods can also hard to be used in complicated matrixes. In this contribution, GO was employed as an efficient signal-to-background enhancer in order to achieve the high sensitivity. Meanwhile, the aptamer of coralyne, poly adenosine (poly A) [19–22], was used as a selective recognition element for strong binding of the coralyne in this system. Base on the emulative bindings of GO and coralyne to the aptamer, the coralyne could be quantificationally detected by the variation of the fluorescence intensity. This method is highly sensitive and selective, and has been applied to practical analysis in complicated matrixes.

2. Experimental

2.1. Chemicals and materials

GO sheets were synthesized according to a modified Hummers method [23,24]. Coralyne chloride, 2-(4-amidinophenyl)-6-indolecarbamidine dihydrochloride (DAPI), sybr green1(SG 1), and acridine orange (AO) were commercially available from Sigma (St. Louis, USA). Berberine chloride and jatrorrhizine chloride were purchased from the National Institute for the Control of Pharmaceutical and Biological Products (Beijing, China). All of the oligonucleotides were synthesized by Shanghai Sangon Biotechnology Co., Ltd. (Shanghai, China). The sequences of the DNA used in this work were listed as follows: 5′–TAMRA-AAA AAA AAA AAA AAA A-3′ (the aptamer of coralyne, TAMRA-aptamer), 5′–TAMRA-CTT ACG GTG GGG CAA TT-3′ (DNA 2), 5′–TAMRA-AGC TTC TTT CTA ATA CGG CTT ACC-3′ (DNA 3), 5′–GCG AGT GTT AAA AGA GAC CAT CAA TGA GCT CGC-TAMRA-3′ (DNA 4), 5′–FAM-ACT CCT GGG GGA GTA TAT AAT-3′ (DNA 5). Phosphate buffer (PB, 0.2 mol L^{-1}) was used to control the acidity of the solution. Mili-Q purified water (18.2 MΩ cm) was used throughout the experiment.

2.2. Experimental instrumentation

Fluorescence spectra and fluorescence anisotropy were measured with an F-2500 fluorescence spectrophotometer (Hitachi, Japan). The Jacso J-810 circular dichroism (CD) spectropolarimeter (Japan) was employed to confirm the conformation of the aptamer. The fluorescence images were recorded with an IX81 microscope with a 40 × objective (Olympus, Japan). A QL-901 vortex mixer (Haimen, China) was employed to mix the solution. A high-speed TGL-16 M centrifuge (Hunan, China) was used during the purification of GO and uric samples.

2.3. Synthesis of graphene oxide

The details for the synthesis of GO sheets were identical with our previous works [6,25], which is also shown in the Supporting Information.

2.4. Experimental measurements

A certain concentration of coralyne was added to the mixture of 10 nmol L^{-1} TAMRA-aptamer, 20 mmol L^{-1} PB buffer, and 8 μg mL^{-1} GO at pH 7.4 (total volume, 500 μL). After 20 min at room temperature, the mixture was measured on the F-2500 fluorescence spectrophotometer with an excitation wavelength of 550 nm.

For the practical detection of uric samples, a series of uric samples were firstly centrifuged at 10000 rpm for 20 min to remove the possible aggregates and then diluted for 50 times. The testing samples were prepared by mixing uric samples with standard coralyne solution. The samples (50 μL) were then added to the mixture of GO and TAMRA-aptamer (total volume, 500 μL) containing 10 nmol L^{-1} TAMRA-aptamer, 20 mmol L^{-1} PB (pH 7.4), and 8 μg mL^{-1} GO.

For the experiments of cell imaging, human bone marrow neuroblastoma (SK-N-SH) cells were firstly incubated in medium supplemented with 10% fetal bovine serum at 37 °C under 5% CO_2. Then, the cells were cleaved by trypsin and replaced onto 18 mm glass coverslips in a 24-well tissue culture plate and allowed them to grow for 24 h. Then, coralyne, GO, and TAMRA-aptamer (or their complex) were added into the medium for incubation. After 3 h, the cells were washed thrice in PBS buffer, fixed with 4% p-formaldehyde for 30 min, and mounted on microscope slides for the imaging.

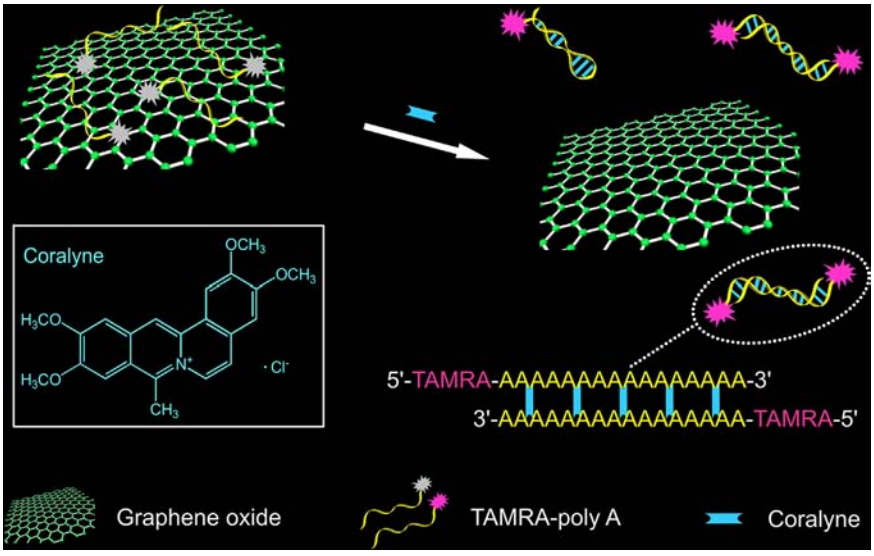

Fig. 1. Schematic illustration showing the OSMs-participating interaction between aptamer and GO, in which coralyne is a typical example of OSMs. Based on this strategy, coralyne can be detected by the turn-on fluorescence after the recognition of its aptamer.

3. Results and discussion

3.1. Design strategy

Fig. 1 illustrates the present strategy for the detection of OSMs based on the on–off–on fluorescence, where the fluorescence of the dye-labeled aptamer can be effectively quenched by interacting with GO, however, it will be turned on after the stronger binding between the aptamer and its target. Specifically, TAMRA-labeled poly A, the aptamer of coralyne, was firstly absorbed onto the surfaces of GO through π–π stacking interaction between the nucleobases and the hexagonal cells of graphene, as well as the weak hydrogen-bonding interactions between primary amines of the bases and oxygen-related groups of the GO sheets [10]. In this case, the fluorescence of TAMRA-aptamer could be quenched by GO owing to the long-range resonance energy transfer (LrRET), where TAMRA-aptamer is the energy donor and GO is the energy acceptor [7,15]. LrRET has been proven to have much higher RET efficiency than that of Föster resonance energy transfer (FRET), because the rate of RET between the dye and graphene has an R^{-4} dependence, wherein R is the relative distance between the donor and acceptor [7,15,26]. Thus, this GO-based LrRET platform could effectively improve the signal-to-background ratio, resulting in high sensitivity of this method.

3.2. Sensor performance

GO sheets used in this work were prepared by a modified Hummers method, which had been demonstrated to have single to a few layers [6,23,24]. In order to demonstrate the feasibility of our designed strategy for the detection of OSMs, we firstly studied the fluorescence features of the OSMs-participating interaction between TAMRA-aptamer and GO. Fig. 2a showed that the fluorescence intensity of TAMRA-aptamer (centered at 582 nm) gradually decreased with increasing the concentration of GO, indicating that TAMRA-aptamer could be easily adsorbed onto the surface of GO sheets [8,13]. The quenching efficiency of the TAMRA-labeled poly (A_{16}) could reach 96% with the addition of 8 μg mL^{-1} of GO. Thus, the strong quenching capability of GO to TAMRA due to their LrRET in this system could result in the low background signal of fluorescence, further improving the signal-to-background ratio of this method. However, with the addition of a series concentrations of coralyne into the mixture of GO and TAMRA-aptamer, a sequential increase of the fluorescence emission could be observed (Fig. 2b). The efficiency of fluorescence restoration could get 90% with the addition of only 500 nmol L^{-1} of coralyne. The relative fluorescence intensity (F/F_0) is linearly proportional to the concentrations of coralyne in the range of 10 −700 nmol L^{-1} (Fig. 2b, insert), suggesting that the detection of coralyne with high sensitivity and in a broad range of concentrations could be achieved by the present analytical method.

Since the binding energies of DNA nucleobases with graphene follow the order of G > A > C≈T [27], the TAMRA-aptamer containing 16 A used in the present work could firmly bind to the surfaces of GO sheets. To evaluate whether the sequence of this aptamer is specific to coralyne, other four dye-labeled DNA with random sequences were employed as comparison groups for the detection of coralyne. It was found that the fluorescence quenching efficiencies of TAMRA- or FAM-labeled DNA with random sequences were much lower than that of TAMRA-aptamer, clarifying that distinct binding affinity of different DNA sequences to GO sheets (Supporting Information, Fig. S1). With the addition of coralyne, the efficiency of fluorescence restoration of TAMRA-aptamer-GO complex was also stronger than that of other four DNA with random sequences. The highest ratio of fluorescence restoration over quenching by using the specific aptamer, poly (A_{16}), demonstrated that it was an ideal platform for the sensitive and selective detection of coralyne.

Fluorescence anisotropy (FA), a powerful and robust parameter to investigate molecular interactions by the differences in orientation and rotational correlation time of fluorophores [28], was measured to clarify the interactions of GO and TAMRA-aptamer as well as the GO-aptamer complex with coralyne. Fig. 3a shows that TAMRA-aptamer rotated at a certain rate owing to its relatively small size in solution. After the binding with GO, however, the FA value dramatically enhanced. This result was attributed to the decrease of the rotational rate of TAMRA-aptamer-GO complex compared with that of free TAMRA-aptamer in solution. It also indicated that strong interaction of GO and TAMRA-aptamer assuredly occurred, and the degree of the FA change depended on the strength of their binding. With the addition of a sequential increase of coralyne into the TAMRA-aptamer-GO complex, however, the decreased FA value was observed. Previous reports have demonstrated that coralyne can

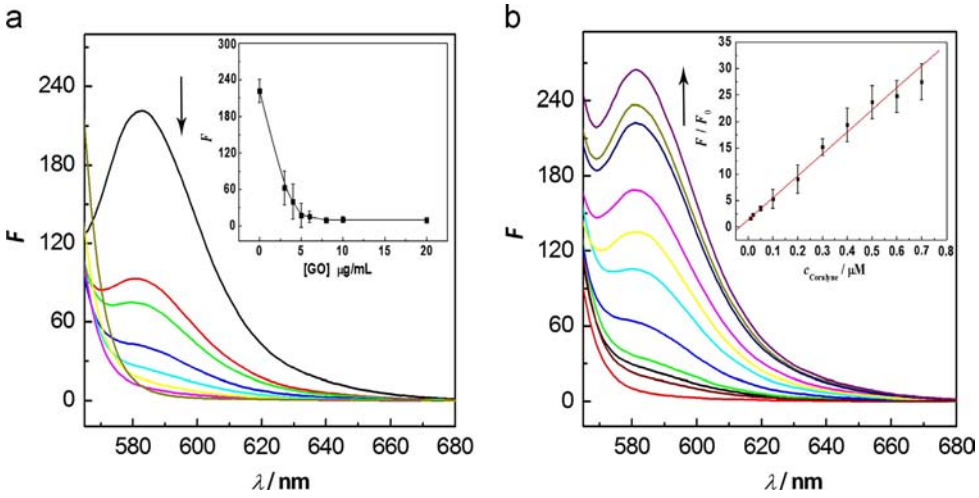

Fig. 2. Spectrofluorometric features of binding chemistry of GO and aptamer in the absence and presence of coralyne. (a) Fluorescence quenching of the TAMRA-aptamer of coralyne with a addition of different concentrations of GO (3, 4, 5, 6, 8, 10, and 20 μg mL^{-} (from top to down); (b) fluorescence restoration with the addition of different concentrations of coralyne (from bottom to the top trace: 0, 10, 20, 50, 100, 200, 300, 400, 500, 600, and 700 nmol L^{-1}). The inset shows the corresponding linear dependence of F/F_0 (relative fluorescence intensity, wherein F_0 and F are the fluorescence intensity in the absence and presence of coralyne, respectively) on the concentration of coralyne. Error bars in the inset were obtained from three parallel experiments. The concentrations of GO and TAMRA-aptamer were 8 μg mL^{-1} and 10 nmol L^{-1}, respectively.

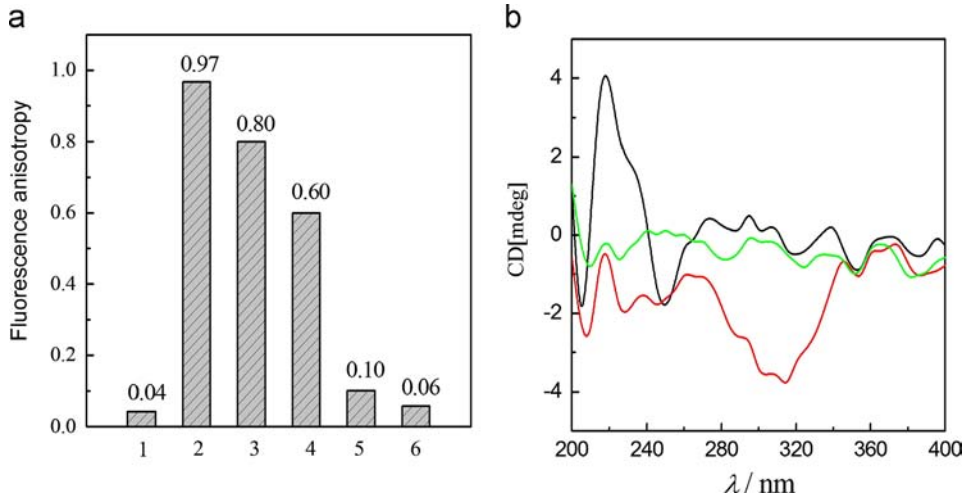

Fig. 3. Conformation change of aptamer during the interaction. (a) Fluorescence anisotropy of (1) TAMRA-aptamer, (2) TAMRA-aptamer-GO complex, and (3–6) the mixture of TAMRA-aptamer-GO complex and coralyne. The concentrations of coralyne: (3) 20 nmol L^{-1}, (4) 60 nmol L^{-1}, (5) 100 nmol L^{-1}, and (6) 500 nmol L^{-1}. The concentrations of GO and TAMRA-aptamer were 8 μg mL^{-1} and 10 nmol L^{-1}, respectively. (b) CD spectra of 1 μmol L^{-1} TAMRA-aptamer (black, top trace), 40 μmol L^{-1} coralyne (green, medial trace) and the mixture of TAMRA-aptamer and coralyne (red, bottom trace). (For interpretation of the references to color in this figure legend, the reader is referred to the web version of this article.)

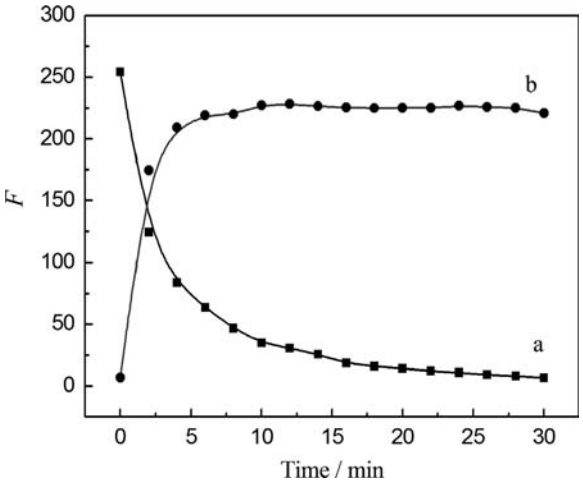

Fig. 4. Kinetic curves of fluorescence show the processes for the loading/release of the TAMRA-aptamer on/off the GO sheets in the present system. (a) Fluorescence quenching process of the TAMRA-aptamer as binding to GO in 30 min; (b) Fluorescence restoration process of TAMRA-aptamer when it released from GO sheets coursed by the recognition of coralyne in 30 min. The concentrations of coralyne, aptamer, GO, and PB buffer solution (pH 7.4) were 500 nmol L^{-1}, 10 nmol L^{-1}, 8 μg mL^{-1}, and 20 mmol L^{-1}, respectively. Fluorescence excitation is at 550 nm and the emission is at 582 nm.

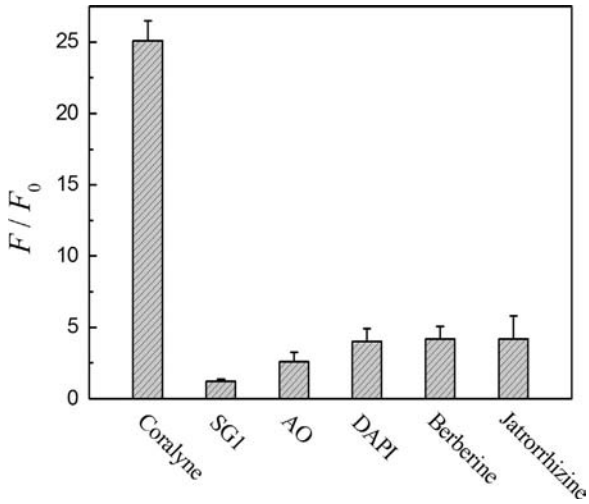

Fig. 5. Selectivity of the present method for the detection of coralyne. Concentrations: coralyne and the compared reagents, 500 nmol L^{-1}; aptamer, 10 nmol L^{-1}; GO, 8 μg mL^{-1}; PB buffer (pH 7.4), 20 mmol L^{-1}.

strongly bind to the DNA sequences with poly A and form the double-stranded structure [19–22]. Here, CD spectra were also measured to clarify whether the configuration of TAMRA-aptamer would change before and after its interaction with coralyne. Fig. 3b clearly revealed the formation of double-stranded structure after the interaction between TAMRA-aptamer and coralyne. Thus, the dramatical change of FA value with the addition of coralyne here was attributed to the coralyne-induced configuration change of the TAMRA-aptamer, and then made it release from the surfaces of GO sheets owing to the formation of rigid double-stranded structure [29].

It was found that either the fluorescence quenching of TAMRA-aptamer directed by GO or the fluorscene restoration through the addition of coralyne were both time-dependent (Fig. 4). On the one hand, the process of fluorescence quenching was fairly fast, with nearly 90% within 10 min after the addition of GO in the TAMRA-aptamer solution. On the other hand, the degree of fluorescent restoration could reach about 90% within only 5 min with the addition of 500 nmol L^{-1} coralyne. These results implied that both the adsorption of TAMRA-aptamer on GO sheets and the release of the double-stranded structure of TAMRA-aptamer-coralyne complex from GO sheets were dynamic and rapid processes, which was conducive to the achievement of rapid detection of coralyne.

In order to obtain the optimal experimental condition for the detection of coralyne, the amount of GO, pH value of the system, and the order of regents added were further investigated. The results showed that optimal efficiency of fluorescence restoration over quenching without/with coralyne was obtained when the concentration of GO suspension was 5–10 μg mL^{-1} and the pH value of the system was in the range of 7.0–8.0 (Supporting Information, Fig. S2 and Fig. S3). In addition, the order of regents added had no significant effect on the fluorescence quenching and restoration (Supporting Information, Fig. S4). In other words, this method is not sensitive to the environmental conditions, and can

be a promising strategy for the detection of coralyne in complex matrixes.

3.3. Selectivity for the detection

To test the selectivity of this strategy, three typical DNA intercalating ligands, SG 1, AO, and DAPI, as well as two drugs with similar molecular structures as coralyne, berberine and jatrorrhizine, were tested as parallel controls with the standard procedure. Fig. 5 shows that the F/F_0 value in the presence of coralyne was more than eight times than that the other three double-stranded DNA intercalating ligands and two drugs with similar structures as coralyne. The result demonstrated that the present off–on fluorescence probe is highly selective to coralyne, which is promising to use in some complicated matrixes.

3.4. Analytical application

In order to demonstrate the feasibility of this analytical method in complicated matrixes, it was then applied to uric samples with the addition of trace amount of coralyne. The results revealed that the recoveries for the detection were between 96.0–97.3% under the optimal condition (Supporting Information, Table S1), indicating that the present method is reliable and practical.

3.5. Cell imaging

Except for the detection of coralyne in uric samples, we further investigated whether the present strategy could be applied for the detection of coralyne in biological media. In such a case, we conducted this GO-based energy transfer platform in cell imaging. As shown in Fig. 6(a–c), the TAMRA-aptamer could penetrate

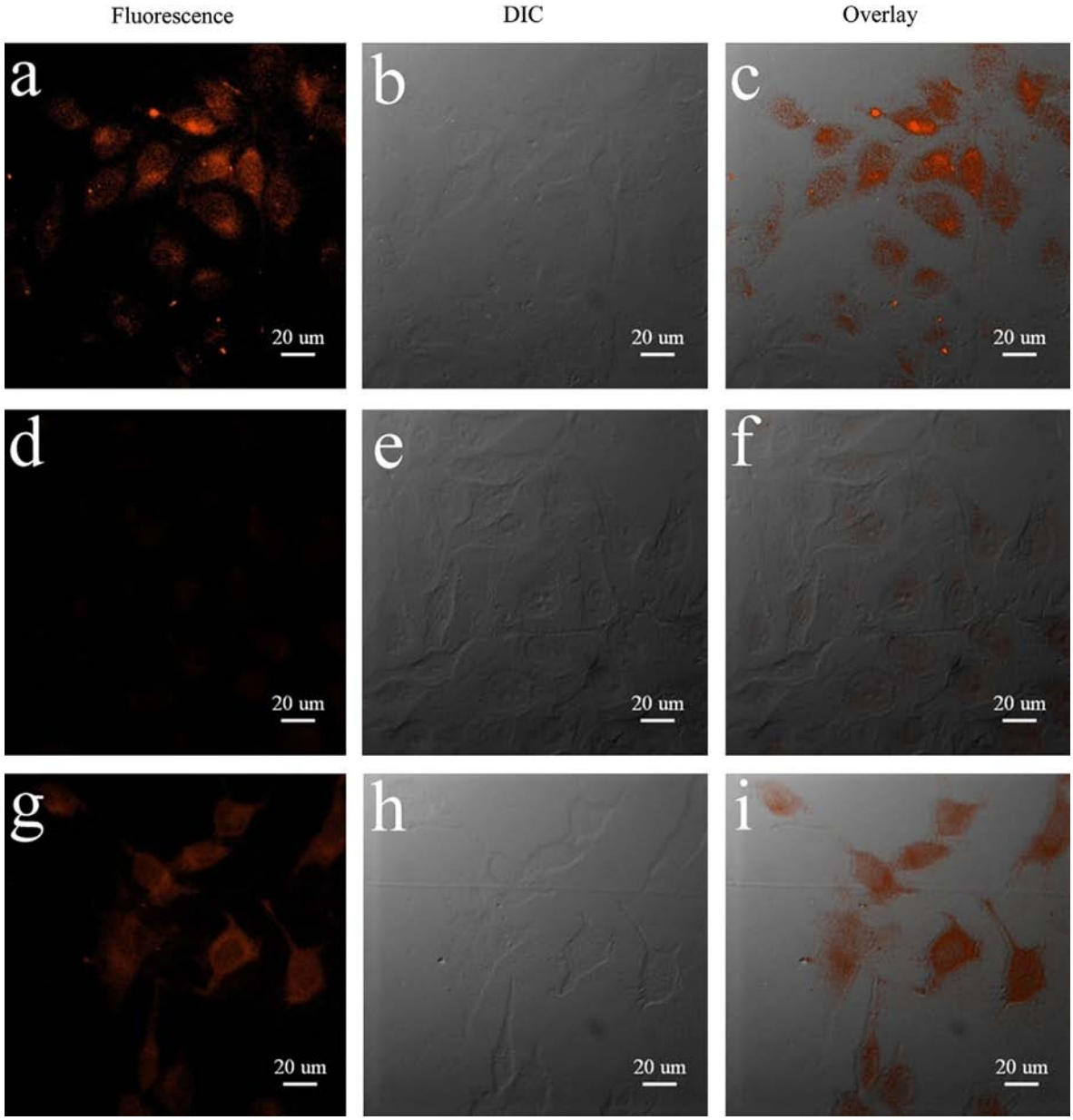

Fig. 6. Fluorescence images showing the interaction of coralyne with TAMRA-aptamer-GO complex in living cells. (a–c) TAMRA-aptamer, (d–f) TAMRA-aptamer-GO complex, and (g–i) TAMRA-aptamer-GO complex interacted with coralyne. Conditions: aptamer, 100 nmol L^{-1}; GO, 30 μg mL^{-1}; coralyne, 5 μmol L^{-1}; PB buffer (pH 7.4), 20 mmol L^{-1}. The mixture was incubated up to 3 h at 37 °C before the imaging. Scale bars, 20 μm.

through the cellular membrane of living cells, and red fluorescence of dye could be observed clearly. However, the fluorescence was quenched distinctly with the addition of GO (Fig. 6(d–f)), which indicated that the aptamer could also bind to GO in cells. Then, the dramatic fluorescence restoration of the aptamer was observed after it interacted with coralyne (Fig. 6(g–i)), which was attributed to the release of TAMRA-aptamer from GO sheets and thus restraint of the LrRET between the dye and GO. All of the fluorescence images demonstrated that the LrRET between the dye and GO was able to occur in living cells with high quenching efficiency, and the fluorescence also could be restored via the recognition of the aptamer and its target. Thus, the present platform could be a promising candidate for the transport and detection of drugs in biological systems.

4. Conclusions

In conclusion, we designed a simple, rapid, highly sensitive and selective biosensor for the detection of OSMs based on the interactions among GO, aptamer and its target. Due to the effective LrRET between graphene and organic dyes, GO has strong power to quench the fluorescence of the TAMRA-aptamer. As a result, low background signal for the detection and thus the high sensitivity of the analytical method has been achieved. Moreover, specific recognition of the aptamer and its target made the present method excellent strategy for the highly selective detection of OSMs. Therefore, this analytical method has been successfully applied for the detection of coralyne in relatively complicated matrixes such as uric samples and cells. Based on the effective LrRET and molecular recognition interactions, this novel biosensor composed of graphene and aptamer can be extended to a wide range of areas related to sensing, environmental monitoring, pharmaceutical analysis, and biological imaging.

Acknowledgments

This work was supported by the National Natural Science Foundation of China (NSFC, 21035005).

Appendix A. Supporting information

Supplementary data associated with this article can be found in the online version at http://dx.doi.org/10.1016/j.talanta.2013.03.013.

References

[1] D.A. Skoog, D.M. West, F.J. Holler, New York: Saunders College Publishing, Fundamentals of analytical chemistry, 5th Edition, 1988.
[2] P.R. Selvakannan, A. Swami, D. Srisathiyanarayanan, P.S. Shirude, R. Pasricha, A. B. Mandale, M. Sastry, Langmuir 20 (2004) 7825–7836.
[3] H. Szelke, S. Schubel, J. Harenberg, R. Kramer, Chem. Commun. 46 (2010) 1667–1669.
[4] Z.D. Liu, P.P. Hu, H.X. Zhao, Y.F. Li, C.Z. Huang, Anal. Chim. Acta 706 (2011) 171–175.
[5] H. Chang, L. Tang, Y. Wang, J. Jiang, J. Li, Anal. Chem. 82 (2010) 2341–2346.
[6] Y. Wang, S.J. Zhen, Y. Zhang, Y.F. Li, C.Z. Huang, J. Phys. Chem. C 115 (2011) 12815–12821.
[7] Y. Zhang, Y. Liu, S.J. Zhen, C.Z. Huang, Chem. Commun. 47 (2011) 11718–11720.
[8] H. Jang, Y.-K. Kim, H.-M. Kwon, W.-S. Yeo, D.-E. Kim, D.-H. Min, Angew. Chem. Int. Ed. 49 (2010) 1–6.
[9] C.-H. Lu, H.-H. Yang, C.-L. Zhu, X. Chen, G.-N. Chen, Angew. Chem. Int. Ed. 48 (2009) 4785–4787.
[10] S. He, B. Song, D. Li, C. Zhu, W. Qi, Y. Wen, L. Wang, S. Song, H. Fang, C. Fan, Adv. Funct. Mater. 19 (2009) 1–7.
[11] N. Mohanty, V. Berry, Nano Lett. 8 (2008) 4469–4476.
[12] Y. Wang, Z. Li, D. Hu, C.-T. Lin, J. Li, Y. Lin, J. Am. Chem. Soc. 132 (2010) 9274–9276.
[13] Y. Wen, F. Xing, S. He, S. Song, L. Wang, Y. Long, D. Li, C. Fan, Chem. Commun. 46 (2010) 2596–2598.
[14] X. Yang, X. Zhang, Z. Liu, Y. Ma, Y. Huang, Y. Chen, J. Phys. Chem. C 112 (2008) 17554–17558.
[15] S.J. Zhen, L.Q. Chen, S.J. Xiao, Y.F. Li, P.P. Hu, L. Zhan, L. Peng, E.Q. Song, C. Z. Huang, Anal. Chem. 82 (2010) 8432–8437.
[16] T.-C. Chiu, C.-C. Huang, Sensors 9 (2009) 10356–10388.
[17] W.D. Wilson, A.N. Gough, J.J. Doyle, M.W. Davidson, J. Med. Chem. 19 (1976) 1261–1263.
[18] F. Xing, G. Song, J. Ren, J.B. Chaires, X. Qu, FEBS Lett. 579 (2005) 5035–5039.
[19] X. Xu, J. Wang, F. Yang, K. Jiao, X. Yang, Small 5 (2009) 2669–2672.
[20] Z. Lv, H. Wei, B. Li, E. Wang, Analyst 134 (2009) 1647–1651.
[21] Ö.P. Çetinkol, N.V. Hud, Nucleic Acids Res. 37 (2009) 611–621.
[22] J. Ren, J.B. Chaires, Biochemistry 38 (1999) 16067–16075.
[23] W.S. Hummers, R.E. Offeman, J. Am. Chem. Soc. 80 (1958) 1339 1339.
[24] Y. Xu, H. Bai, G. Lu, C. Li, G. Shi, J. Am. Chem. Soc. 130 (2008) 5856–5857.
[25] Y. Wang, P. Zhang, C.F. Liu, L. Zhan, Y.F. Li, C.Z. Huang, RSC Adv. 2 (2012) 2322–2328.
[26] R.S. Swathi, K.L. Sebastian, J. Chem. Phys. 130 (2009) 086101.
[27] N. Varghese, U. Mogera, A. Govindaraj, A. Das, P.K. Maiti, A.K. Sood, C.N.R. Rao, Chem. Phys. Chem. 10 (2009) 206–210.
[28] M.E. McCarroll, F.H. Billiot, I.M. Warner, J. Am. Chem. Soc. 123 (2001) 3173–3174.
[29] A.J. Patil, J.L. Vickery, T.B. Scott, S. Mann, Adv. Mater. 21 (2009) 3159–3164.